Exploring the Effect of Variability of Urban Systems Characteristics in the Network Capacity

by

Burak Boyacı

School of Architecture, Civil and Environmental Engineering

Urban Transport Systems Laboratory

Ecole Polytechnique Fédérale de Lausanne (EPFL)

GC C2 399, Station 18, 1015 Lausanne, Switzerland

Phone: +41-21-69-35397

e-mail: burak.boyaci@epfl.ch

Nikolas Geroliminis*

School of Architecture, Civil and Environmental Engineering

Urban Transport Systems Laboratory

Ecole Polytechnique Fédérale de Lausanne (EPFL)

GC C2 389, Station 18, 1015 Lausanne, Switzerland

Phone: +41-21-69-32481, Fax: +41-21-69-35060

e-mail: nikolas.geroliminis@epfl.ch

*Corresponding author

5400 words + 8 figures + 0 tables

For Presentation only

90th Annual Meeting

Transportation Research Board

Washington, D.C.

January 2011

revised version

ABSTRACT

Mobility and transportation are two of the leading indicators of economic growth of a society. As cities around the world grow rapidly and more people and modes compete for limited urban space to travel, there is an increasing need to understand how this space is used for transportation and how it can be managed to improve accessibility for everyone. In a recent paper, Daganzo and Geroliminis (*1*) explored the connection between network structure and a network's MFD for urban neighborhoods with cars controlled by traffic signals and derived an analytical theory for the MFD using Variational Theory. Information needed to estimate this network MFD's are average network (total length of roads in lane-km, number of lanes, length of links), control (signal offsets, green phase and cycle time) and traffic (free flow speed, congested wave speed, jam density, capacity) characteristics. However in previous studies, Variational Theory has been applied only in cities with deterministic values of the above variables for the whole network and by ignoring the effect of turns. In our study we are aiming to generate an MFD for streets with variable link lengths and signal characteristics and understand the effect of variability for different cities and signal structures. Furthermore, this variability gives the opportunity to mimic the effect of turning movements and heterogeneity in drivers' behavior. This will be a key issue in planning the signal regimes such a way that maximizes the network capacity and/or the density range of the capacity.

INTRODUCTION

The first theoretical proposition of a macroscopic relationship between average network flow and density with an optimum accumulation belongs to Godfrey (*2*). Earlier studies looked for macroscale traffic patterns in data of lightly congested real-world networks (Ardekani & Herman (*3*); Olszewski et al. (*4*)) or in data from simulations with artificial routing rules and static demand (Mahmassani et al. (*5*); Mahmassani & Peeta (*6*)). However, the data from all these studies were too sparse or not investigated deeply enough to demonstrate the existence of an invariant macroscopic relation for real urban networks. Later, Daganzo (*7*) conjectured (as part of an urban traffic dynamics model) that a well-defined relationship between flow and density must arise if a network is "uniformly loaded" in space and demand changes slowly with time.

The empirical verification of its existence with dynamic features is recent (*8*) (*9*). The experiments and simulations in these references suggest that under some conditions this macroscopic relation is indeed a reproducible curve named as the 'Macroscopic Fundamental Diagram' (MFD). These references also showed that the MFD is a property of the network infrastructure and control and not of the demand, i.e. space-mean flow is maximum for the same value of vehicle density independently of time-dependent origin-destination tables. Despite these and other recent findings for the existence of well-defined macroscopic fundamental diagrams (MFDs) for urban areas, it is not obvious whether the MFDs would be universal or network-specific. More real-world experiments are needed to identify the types of networks and demand conditions, for which invariant MFD's with low scatter exist.

To evaluate topological or control-related changes of the network (e.g. a re-timing of the traffic signals or a change in infrastructure), Daganzo and Geroliminis (*1*) and Helbing (*10*) have derived analytical theories for the urban fundamental diagram, using a density-based and a utilization-based approach respectively. The first reference proved, using Variational Theory (*7*), that an MFD must arise for single-route networks with a fixed number of vehicles in circulation (periodic boundary conditions and no turns). The same reference also gives explicit formulae for the single-route MFD with deterministic topology, control and traffic characteristics (i.e. all intersections have common control patterns, the length of its links and their individual fundamental diagrams are all the same. The reference conjectured that these MFD formulae should approximately expected to hold for homogeneous, redundant networks with slow-changing demand.

In this paper we provide several extensions and refinements of the analytical model for an MFD. We explore how network parameters (topology and signal control) affect two key characteristics of an MFD, (i) the network capacity and (ii) the density range for which the network capacity is maximum. We also investigate how sensitive are these two characteristics in small changes of the parameters. Afterwards, we relax the deterministic character of the parameters and we investigate how variations in the signal offsets and the link lengths affect network capacity and density range. These results can be utilized to develop efficient control strategies for a series of signalized intersections as these variations can describe not only differences in network parameters, but also different characteristics in driver behavior. Later, we imitate the effect of incoming turns in a long arterial and we show that these turns can significantly decrease the network capacity. To precisely describe all the above phenomena we initially provide some analytical proofs for a simplification of the Variational Theory approach and then we develop a simulator to study the non-deterministic effects.

A NOTE ON VARIATIONAL THEORY

Daganzo and Geroliminis (*1*) used a moving observer method to show that the average flow-density states of any urban street without turning movements must be bounded from above by a concave curve. The section also shows that, under the assumptions of variational theory, this curve is the locus of the possible (steady) traffic states for the street; i.e., it is its MFD.

Their method builds on a recent finding of Daganzo (*7*), which showed that kinematic wave theory traffic problems with a concave flow-density relation are shortest (least cost) path problems. Thus, the centerpiece of variational theory (as is the fundamental diagram for kinematic wave theory) is a relative capacity ("cost") function (CF), $r\left(u\right)$, that describes each homogeneous portion of the street. This function is related to the known FD of kinematic wave theory Q. Physically, the CF gives the maximum rate at which vehicles can pass an observer moving with speed u and not interacting with traffic; i.e., the street's capacity from the observer's frame of reference. Linear CFs correspond to triangular FDs. Daganzo and Geroliminis (*7*) assumed a linear CF characterized by the following parameters: k_0 (optimal density), u_f (free flow speed), κ (jam density), w (backward wave speed), s (capacity), and r (maximum passing rate). CF line crosses points $(u_f, 0)$, $(0, s)$, $(-w, r)$ and has a slope equal to $-k_0$. Other applications of Variational Theory in modeling traffic phenomena can be found in (*11*).

A second element of VT is the set of "valid" observer paths on the (t, x) plane starting from arbitrary points on the boundary at $t = 0$ and ending at a later time, $t_0 > 0$. A path is "valid" if the observer's average speed in any time interval is in the range $[-w, u_f]$. If $\mathcal{P}$ is one such path, $u_{\mathcal{P}}$ be the average speed for the complete path, and $\Delta\left(\mathcal{P}\right)$ is the path's cost which is evaluated with $r\left(u\right)$, $\Delta\left(\mathcal{P}\right)$ bounds from above the change in vehicle number that could possibly be seen by observer $\mathcal{P}$. Thus, the quantity:

$$\lim_{t_o \to \infty} \inf_{\mathcal{P}} \left\{\Delta\left(\mathcal{P}\right) : u_{\mathcal{P}} = u\right\} / t_o \tag{1}$$

is an upper bound to the average rate at which traffic can overtake any observer that travels with average speed u for a long time. Note that (1) is a shortest path problem, and that $R\left(0\right)$ is the system capacity. Building on Equation (1), Daganzo and Geroliminis (*1*) proved that a ring's MFD with periodic characteristics in time and space (traffic signals every L meters with common green duration G and cycle C and no turns), $Q = Q\left(k\right)$, is concave and given by Equation (2). Figure (1a) illustrates that Equation (2) is the lower envelope of the 1-parameter family of lines on the (k, q) plane defined by $q = ku + R\left(u\right)$ with u as the parameter. Note this equation also describes the passing rate of an observer moving with constant speed u in a stationary traffic stream with flow q and density k. The main difference is that traffic signals create non-stationary conditions as vehicles stop at traffic signals and this relation does not apply in all cases. We call these lines "cuts" because they individually impose constraints of the form: $q \leq ku + R\left(u\right)$ on the macroscopic flow-density pairs that are feasible on a homogeneous street.

$$q = \inf_{u} \left\{ku + R\left(u\right)\right\} \tag{2}$$

Because evaluating $R\left(u\right)$ in Equation (2) for all u can be tedious, Daganzo and Geroliminis (*1*) proposed instead using three families of "practical cuts" that jointly bound the MFD from above, albeit not tightly. It has been shown (*7*) that for linear CF's, an optimal path always exists that is piece-wise linear: either following an intersection line or else slanting up or down with slope u_f or $-w$. The practical cuts are based on observers that can move with only 3 speeds:

$u = u_f$, 0, or w and stop at intersections during red times and possibly during green periods as well. Recall that an observer's cost rate (maximum passing rate) is $q_B(t)$ if the observer is standing at intersection with capacity $q_B(t) \leq s$ and otherwise it is given by a linear CF, i.e. it is either 0, s or r depending on the observer's speed.

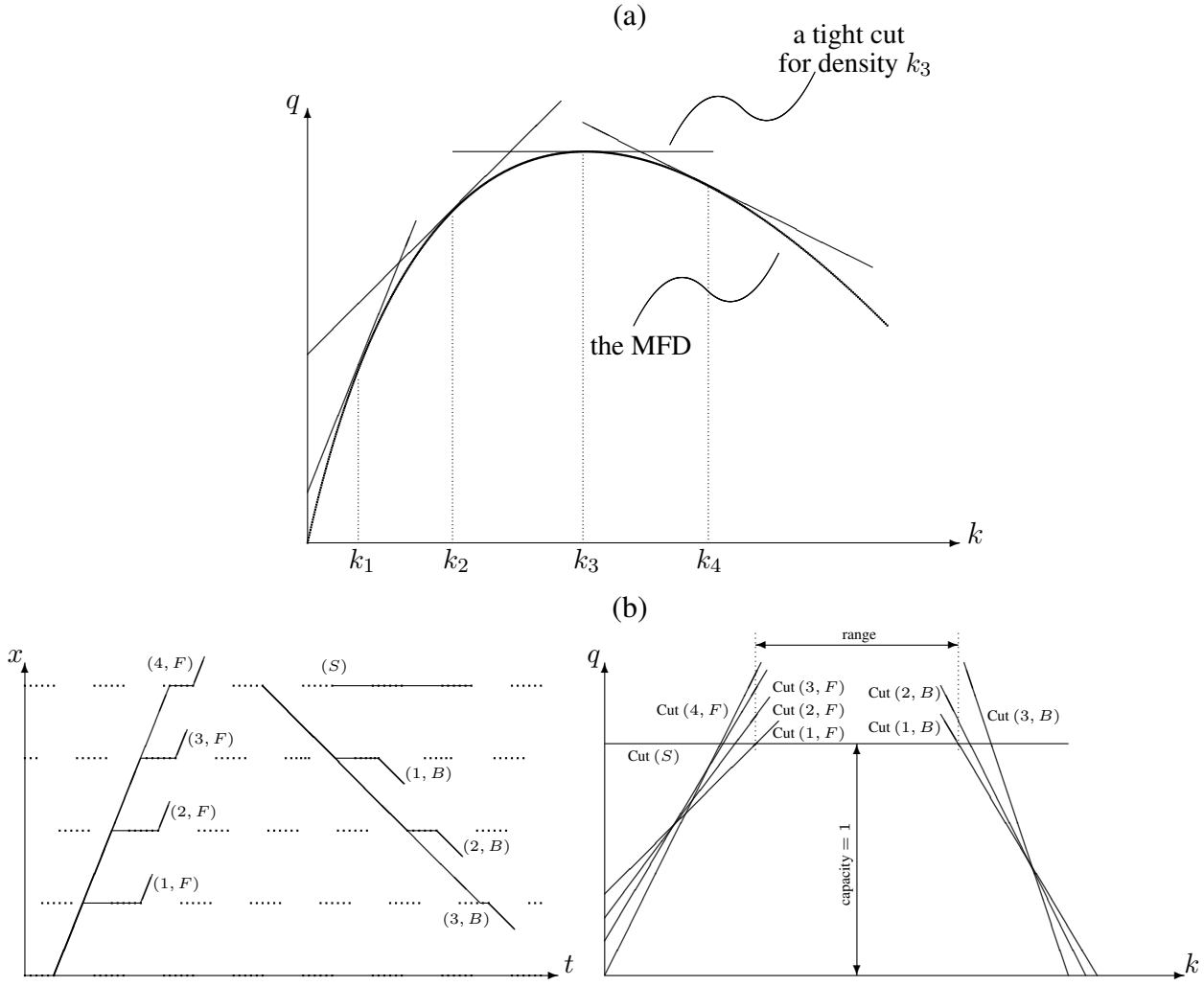

Figure 1: The MFD defined by a 1-parameter family of "cuts" (*1*) and both forward, backward and stationary observers

Figure (1b) provides an explanation how the "practical cuts" are estimated for a series of intersections with common length and signal settings (green G, cycle C and offset δ). For offset is the time difference between the starting of the green phase for two consecutive signals. Case $(4, F)$ shows the fastest moving observer, who runs with speed u_f and stops only at red phases once every 4 signals. No vehicles are passing her, the first "cut" crosses the $q - k$ plane at $(0, 0)$ and has a slope equal to the average speed of the observer. The 2nd observer $(3, F)$ still runs at u_f but stops during the green period every third signal. Thus, she has a smaller average speed and vehicles are passing her at rate s when waiting in green phases. This passing rate is shown in the second "cut" as the constant of the line that crosses axis q at $q > 0$. The 3rd observer $(2, F)$ stops in every two

signals whereas the fourth $(1, F)$ stops in every signal, while the fifth observer named as (S) is the stationary observer with zero speed. Cases $(3, B)$-$(1, B)$ show the backward moving observers, who are passed at rate r when moving in the opposite direction and at rate s when waiting in green phases. The lower envelope of all these "cuts" produces the MFD.

The authors conjectured that the following regularity conditions should ensure a good analytical approximation of the MFD: (i) a steady and distributed demand; (ii) a redundant network ensuring that drivers have many route choices and that most links are on many desirable routes; (iii) a homogeneous network with similar links; (iv) links with an approximate FD that is not significantly affected by turning movements when flow is steady. Conditions (i)-(iii) should create a near-equilibrium as in Wardrop (*12*) with similar average speeds on all links; and, since the links are similar, with similar (i.e., optimal) densities too. Condition (iv) implies that the VT method, applied to a single link with many efficient cuts, yields a tight MFD. The estimated MFD (despite its simplistic approach) fits well empirical and simulated data for Yokohama and San Francisco, two networks that only roughly meet the regularity conditions.

DETERMINISTIC

In this part of the paper, we will show that, the range of an MFD graph created by variational theory can be found analytically for the case where $L/u_f + L/w < C$. In Lemma (1) we will find the regions in which there are only one forward and/or backward moving observers. Lemma (2) will prove a mathematical inequality. Lemma (3), proves that the slowest forward and backward moving observers are the two observers which makes the tightest cuts in stationary observer line. We will end up the section with three corollaries which give equations of the ranges for most of the regions. The reader can omit these proofs without loss of continuity.

Lemma 1 *For $L/u_f - nC \leq \delta < L/u_f - G + (1-n)\,C$, the fastest forward moving observer will hit the first red signal which results in one forward moving observer only. Similarly, $nC + G - \frac{L}{w} < \delta \leq -\frac{L}{w} + (n-1)\,C$ shows the regions where the fastest backward moving observer hits the first red. For the remaining regions, there are more than one forward and/or backward moving observers.*

Proof The analytical proof of this lemma is straightforward. It can be done by stating $\gamma^f_{max} = 1$ in the equation:

$$\gamma^f_{max} = 1 + \max\left\{\gamma : \frac{\gamma\,(L/u_f - \delta)}{C} - \left\lfloor \frac{\gamma\,(L/u_f - \delta)}{C} \right\rfloor \leq \frac{G}{C}\right\} \tag{3}$$

and $\gamma^b_{max} = 1$ in the following equation

$$\gamma^b_{max} = 1 + \max\left\{\gamma : \frac{\gamma\,(L/w - \delta_w)}{C} - \left\lfloor \frac{\gamma\,(L/w - \delta_w)}{C} \right\rfloor \leq \frac{G}{C}\right\} \tag{4}$$

which is stated by Daganzo and Geroliminis (*1*). However, it is trivial that for $n \in \mathbb{N}$,

$$\delta - C + G + nC < \frac{L}{u_f} \leq \delta + nC \Rightarrow \frac{L}{u_f} - nC \leq \delta < \frac{L}{u_f} - G + (1-n)\,C \tag{5}$$

the observer will hit the n^{th} cycles red of the second signal and there will only be one forward moving observer. Similarly, for backward moving observers we can say that, for $n \in \mathbb{N}$,

$$nC + G - \frac{L}{w} < \delta \leq -\frac{L}{w} + (n-1)\,C, \tag{6}$$

if there is only one backward moving observer. Obviously if the observers do not hit the first red, there will be at least two observers. □

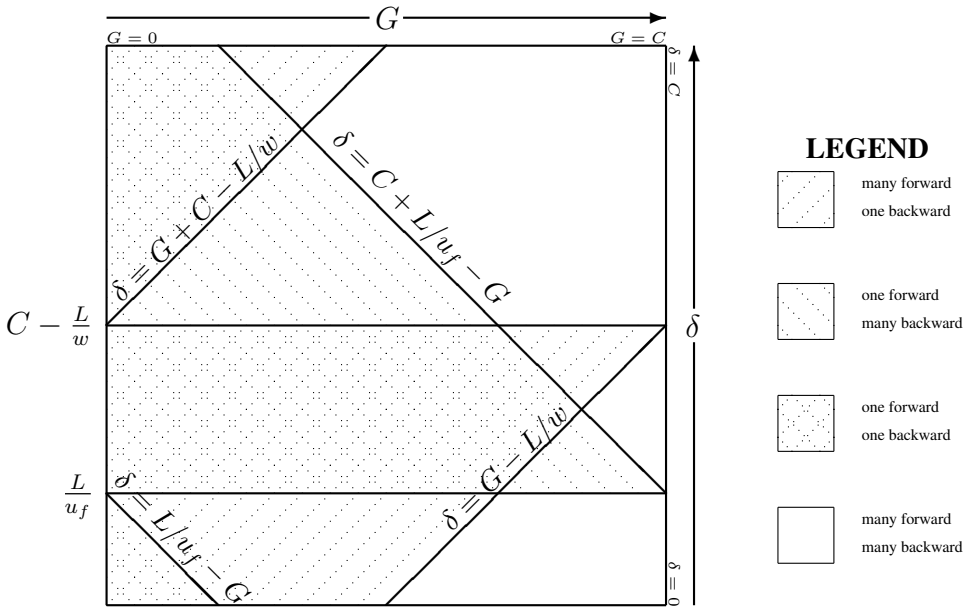

Figure 2: Regions according to Lemma (1) for $L/u_f < C - L/w$.

Lemma 2 *For* $f(x) = \frac{1}{x}\left(\lceil xt \rceil - 1\right)$ *where* $t \in \mathbb{R}$, $f(1) \leq f(x)$ *for* $x \in \mathbb{Z}^+$.

Proof Assume $k < t \leq k+1$ for $k \in \mathbb{Z}$. Note that, this assumption includes all real values of t. From this assumption:

$$k < t \leq k+1 \Rightarrow kx < tx \leq kx+x \Rightarrow \lceil tx \rceil \leq kx+x \Rightarrow f(x) = \frac{1}{x}\left(\lceil tx \rceil - 1\right) \leq k+1-\frac{1}{x}. \tag{7}$$

If we calculate $f(1)$

$$k < t \leq k+1 \Rightarrow \lceil t \rceil = k+1 \Rightarrow f(1) = k, \tag{8}$$

which means $f(1) \leq f(x)$ for $x \in \mathbb{Z}^+$. □

Lemma 3 *For* $L/u_f < C$ *and* $L/w < C$ *slowest forward and backward moving observers has the tightest cuts on the stationary moving observer.*

Proof We provide the proofs separately for the forward and backward moving observers separately. Since both parts use similar steps, in order not to repeat same things, the proof for the forward moving observers will be more detailed than the backward moving observers'.

(FORWARD) We start the proof by writing the equations of the intersection points of stationary observers with the forward moving observers:

$$\text{Cut}\left(\gamma, F\right) \cap \text{Cut}\left(S\right) = \left(q\frac{G-C}{L}\left[\frac{1}{\gamma}\left(\left\lceil\frac{\gamma\left(L/u_f-\delta\right)}{C}\right\rceil-1\right)+\frac{\delta}{C}\right]+\frac{q}{u_f}, q\frac{G}{C}\right) \tag{9}$$

$$\text{Cut}\left(\gamma^f_{max}, F\right) \cap \text{Cut}\left(S\right) = \left(q\frac{G}{L}\left(\frac{1}{\gamma^f_{max}}\left\lceil\frac{\gamma^f_{max}\left(L/u_f-\delta\right)}{C}\right\rceil+\frac{\delta}{C}\right), q\frac{G}{C}\right) \tag{10}$$

Note that, the equations for the fastest forward moving observer and the rest is different. We start by comparing the not-fastest forward moving observers. We seek for γ which gives the tightest cut. This problem can be defined as:

$$\arg\max_{\gamma}\left\{ q\frac{G-C}{L}\left[\frac{1}{\gamma}\left(\left\lceil\frac{\gamma\left(L/u_f-\delta\right)}{C}\right\rceil-1\right)+\frac{\delta}{C}\right]+\frac{q}{u_f} : \gamma\in\mathbb{Z}^+\right\} \tag{11}$$

Since we know that $G<C$, $q>0$ and $L>0$, the above problem is equivalent to:

$$\arg\min_{\gamma}\left\{ \frac{1}{\gamma}\left(\left\lceil\gamma\frac{\left(L/u_f-\delta\right)}{C}\right\rceil-1\right) : \gamma\in\mathbb{Z}^+\right\} \tag{12}$$

which is the same as the function given in Lemma (2). The value of $\gamma\in\mathbb{Z}^+$ that minimizes this function is 1. It is proved that among all not-fastest forward moving observers, slowest one has the tighter cut on stationary observer line.

In order to complete the proof of the forward moving part, we will compare the slowest and the fastest forward moving observers. Define, ε as the differences of the abscissa between the fastest and slowest cuts. More rigorously,

$$\varepsilon = \left\{\text{Cut}\left(1, F\right) \cap \text{Cut}\left(S\right)\right\}_x - \left\{\text{Cut}\left(\gamma^f_{max}, F\right) \cap \text{Cut}\left(S\right)\right\}_x \tag{13}$$

$$\begin{aligned} &= q\left(G-C\right)\left[\frac{1}{L}\left(\left\lceil\frac{\left(L/u_f-\delta\right)}{C}\right\rceil-1\right)+\frac{\delta}{CL}\right]+\frac{q}{u_f} \\ &\qquad -\left[q\frac{G}{\gamma^f_{max}L}\left\lceil\frac{\gamma^f_{max}\left(L/u_f-\delta\right)}{C}\right\rceil+q\frac{G\delta}{CL}\right] \end{aligned} \tag{14}$$

It suffices to show that $\varepsilon\geq 0$. Since, $L/u_f<C$ and $-1<\left(L/u_f-\delta\right)/C<1$, $\lceil\left(L/u_f-\delta\right)/C\rceil$ can take either 1 or 0. For $0<\left(L/u_f-\delta\right)/C<1 \Rightarrow \lceil\left(L/u_f-\delta\right)/C\rceil=1$, after some manipulations:

$$\varepsilon = q\left(\frac{1}{u_f}-\frac{\delta}{L}-\frac{G}{L\gamma^f_{max}}\left\lceil\frac{\gamma^f_{max}\left(L/u_f-\delta\right)}{C}\right\rceil\right). \tag{15}$$

From Equation (3), we can state that,

$$\left\lceil\frac{\gamma^f_{max}\left(L/u_f-\delta\right)}{C}\right\rceil = \left\lfloor\frac{\gamma^f_{max}\left(L/u_f-\delta\right)}{C}\right\rfloor+1 > \gamma^f_{max}\left(\frac{L}{u_f}-\delta\right)/C-\frac{G}{C}+1 \tag{16}$$

which yields to:

$$\varepsilon > q\left(1-\frac{G}{C}\right)\left(\frac{1}{u_f}-\frac{\delta}{L}-\frac{G}{L\gamma^f_{max}}\right) \tag{17}$$

Given that $0 < L/u_f - \delta < C$ and after some manipulations we get,

$$\frac{1}{u_f} - \frac{\delta}{L} - \frac{G}{\gamma^f_{max} L} > \frac{C}{L}\left(\frac{1}{\gamma^f_{max}}\left\lfloor \frac{\gamma^f_{max}\left(L/u_f - \delta\right)}{C}\right\rfloor\right) \geq 0 \tag{18}$$

which shows that $\varepsilon > 0$.

For $\lceil \left(L/u_f - \delta\right)/C \rceil = 0$, after some calculations we get

$$\varepsilon = q\left(1 - \frac{G}{C}\right)\left(\frac{C}{L} - \frac{\delta}{L} + \frac{1}{u_f} - \frac{G}{L\gamma^f_{max}}\right). \tag{19}$$

Similar to Equation (18), we can write:

$$\frac{1}{u_f} - \frac{\delta}{L} - \frac{G}{\gamma^f_{max} L} > \frac{C}{L}\left(\frac{1}{\gamma^f_{max}}\left\lfloor \frac{\gamma^f_{max}\left(L/u_f - \delta\right)}{C}\right\rfloor\right) \geq -\frac{C}{L} \tag{20}$$

If we combine Equations (19) and (20), we get

$$\varepsilon = q\left(1 - \frac{G}{C}\right)\left(\frac{C}{L} - \frac{\delta}{L} + \frac{1}{u_f} - \frac{G}{\gamma^f_{max} L}\right) > 0. \tag{21}$$

(BACKWARD) Let us start by finding the intersection points of backward moving observers and the stationary observer. After some manipulations,

$$\text{Cut}\left(\gamma, B\right) \cap \text{Cut}\left(S\right) = \left(q\frac{C-G}{L}\left[\frac{1}{\gamma}\left(\left\lceil \frac{\gamma\left(L/w - \delta_w\right)}{C}\right\rceil - 1\right) + \frac{\delta_w}{C}\right] + \frac{q}{u_f}, q\frac{G}{C}\right) \tag{22}$$

$$\text{Cut}\left(\gamma^b_{max}, B\right) \cap \text{Cut}\left(S\right) = \left(q\left(\frac{1}{w} + \frac{1}{u_f}\right) - \frac{qG}{L}\left(\frac{\delta_w}{C} + \frac{1}{\gamma^b_{max}}\left\lceil \frac{\gamma^b_{max}\left(\frac{L}{w} - \delta_w\right)}{C}\right\rceil\right), q\frac{G}{C}\right). \tag{23}$$

By using the Lemma (2) and following minimization problem,

$$\arg\min_{\gamma}\left\{\text{Cut}\left(\gamma, B\right) \cap \text{Cut}\left(S\right)\right\}_x = \arg\min_{\gamma}\left\{\frac{1}{\gamma}\left(\left\lceil \frac{\gamma\left(L/w - \delta_w\right)}{C}\right\rceil - 1\right)\right\} \tag{24}$$

we can state that slowest backward moving observer is the tightest among all other not-fastest backward moving observer.

Define ε as the difference between the cuts of slowest and fastest backward moving observers and assume $-C < L/w - C + \delta \leq 0$. After some calculations,

$$\varepsilon = q\left(\frac{1}{w} - \frac{G}{\gamma^b_{max} L}\left\lceil \frac{\gamma^b_{max}\left(L/w - \delta_w\right)}{C}\right\rceil - \frac{G}{L} + \frac{\delta}{L}.\right) \tag{25}$$

After some manipulations by using Equation (4)

$$\varepsilon > q\left(1 - \frac{G}{C}\right)\left(\frac{1}{w} + \frac{\delta}{L} - \frac{G}{\gamma^b_{max} L}\right) \leq 0 \tag{26}$$

which shows that the slowest observer cuts the stationary observer on a point whose abscissa is smaller.

For $0 < L/w - C + \delta < C$, Equation (4) give the inequality

$$\varepsilon > q\left(1 - \frac{G}{C}\right)\left(\frac{1}{w} - \frac{C}{L} + \frac{\delta}{L} - \frac{G}{\gamma^b_{max} L}\right), \tag{27}$$

whose right hand side is non-negative, i.e. $\varepsilon > 0$. □

Corollary 1 *If $L/u_f + L/w < C$, the regions which are bounded by either $\delta < L/u_f$ or $\delta > C - L/w$ and have either one forward and many backward, or many forward and one backward moving observers have a range which is a linear function of δ and G.*

Proof. We should examine four different regions.

I. $\delta > C - L/w$, $\delta < C + L/u_f - G$ and $\delta < G + C - L/w$. In this region there are one forward and many backward observers. Using Equations (10) and (22) range is:

$$\mathrm{R}_{\mathbf{I}} = q\frac{C-G}{L}\left[\frac{1}{\gamma}\left(\left\lceil\frac{\gamma\left(L/w - \delta_w\right)}{C}\right\rceil - 1\right) + \frac{\delta_w}{C}\right] + \frac{q}{u_f} - \left[q\frac{G}{L}\left(\left\lceil\frac{L/u_f - \delta}{C}\right\rceil + \frac{\delta}{C}\right)\right] \tag{28}$$

From the region boundaries given above we can state that:

$$-C < G - C < \frac{L}{u_f} - \delta < \frac{L}{u_f} + \frac{L}{w} - C < 0 \Rightarrow \left\lceil\frac{L/u_f - \delta}{C}\right\rceil = 0 \tag{29}$$

$$0 < \frac{L}{w} - C + \delta < G < C \Rightarrow \left\lceil\frac{\gamma\left(L/w - \delta_w\right)}{C}\right\rceil = 1 \tag{30}$$

By using Equations (29) and (30) we will end up with:

$$\mathrm{R}_{\mathbf{I}} = \frac{q}{L}\left(\frac{L}{u_f} + C - G - \delta\right) \tag{31}$$

II. $\delta > C - L/w$, $\delta > C + L/u_f - G$ and $\delta > G + C - L/w$. Using Equations (9) and (23), and after some manipulations:

$$\mathrm{R}_{\mathbf{II}} = \frac{q}{L}\left(\frac{L}{w} + G - \delta\right) \tag{32}$$

III. $\delta < L/u_f$, $\delta > L/u_f - G$ and $\delta > G - L/w$. In a similar way,

$$\mathrm{R}_{\mathbf{III}} = \frac{q}{L}\left(\frac{L}{w} + \delta - G\right). \tag{33}$$

IV. $\delta < L/u_f$, $\delta < L/u_f - G$ and $\delta < G - L/w \Rightarrow 0 \leq \delta < L/u_f - L/w < 0$ which is a contradiction. This region does not exist. □

Corollary 2 *If $L/u_f + L/w < C$, the regions which are bounded by either $\delta < L/u_f$ or $\delta > C - L/w$ and have more than one forward and backward moving observers, have range equal to* 0.

Proof. The range of regions with more than one forward and backward moving observers is,

$$\mathrm{R}\left(\delta, G\right) = q\frac{G-C}{L}\left(\left\lceil\frac{L/u_f-\delta}{C}\right\rceil + \left\lceil\frac{L/w-C+\delta}{C}\right\rceil - 1\right). \tag{34}$$

We must show that this equation equals to 0 for the cases defined above. In order to do this we need to find values which satisfy

$$\left\lceil\frac{L/u_f-\delta}{C}\right\rceil + \left\lceil\frac{L/w-C+\delta}{C}\right\rceil = 1. \tag{35}$$

$L/u_f < C$ and $0 \leq \delta \leq C$, it is obvious that $-C < L/u_f - \delta < C$. In other words, $\left\lceil\frac{L/u_f-\delta}{C}\right\rceil$ can take only two values, 0 or 1. When the first ceiling function is zero the second one should be one and vice versa. For the first case:

$$0 < \frac{L}{u_f} - \delta < C \text{ and } -C < \frac{L}{w} - C + \delta \leq 0 \Rightarrow \delta < \frac{L}{u_f} \text{ and } \delta < C - \frac{L}{w} \Rightarrow \delta < \frac{L}{u_f}, \tag{36}$$

and similarly for the latter case:

$$-C < \frac{L}{u_f} - \delta \leq 0 \text{ and } 0 < \frac{L}{w} - C + \delta \leq C \Rightarrow \delta > \frac{L}{u_f} \text{ and } \delta > C - \frac{L}{w} \Rightarrow \delta > C - \frac{L}{w}, \tag{37}$$

which is what we want. □

Corollary 3 *If there exist one forward and one backward moving observers, range does not depend on* δ.

Proof. Using Equations (10) and (23) the range for one forward and backward moving observer regions can be formulated as:

$$\mathrm{R}(\delta, G) = q\left(\frac{1}{w}+\frac{1}{u_f}\right) - q\frac{G}{L} - q\frac{G}{L}\left(\left\lceil\frac{L/w-\delta_w}{C}\right\rceil + \left\lceil\frac{L/u_f-\delta}{C}\right\rceil\right). \tag{38}$$

According to Lemma 1, there are two regions with only one forward and backward moving observers, which means there are four intersections that we should investigate.

I. $(\delta < L/u_f - G) \cap (G - L/w < \delta < C - L/w) = G - L/w < \delta < L/u_f - G$:
If we calculate the values of ceiling functions,

$$\frac{L}{w} - C + \delta < \frac{L}{u_f} + G + \frac{L}{w} - C < -G \text{ and } \frac{L}{w} - C + \delta > -C \Rightarrow \left\lceil\frac{L/w-\delta_w}{C}\right\rceil = 0 \tag{39}$$

$$\frac{L}{u_f} - G > \delta \Rightarrow \frac{L}{u_f} - \delta > G \text{ and } \frac{L}{u_f} < C \Rightarrow \frac{L}{u_f} - \delta < C \Rightarrow \left\lceil\frac{L/u_f-\delta}{C}\right\rceil = 1. \tag{40}$$

Then after calculations, our function value $\mathrm{R}_{\mathbf{I}}(\delta, G)$ will be,

$$\mathrm{R}_{\mathbf{I}}(\delta, G) = q\left(\frac{1}{w}+\frac{1}{u_f}-\frac{2G}{L}\right) \tag{41}$$

II. $(\delta < L/u_f - G) \cap (\delta > C - L/w + G) = \emptyset$ since $L/u_f - G \not> C - L/w + G$

III. $(L/u_f < \delta < L/u_f + C - G) \cap (G - L/w < \delta < C - L/w)$ After some manipulations, we will end up with:

$$\mathrm{R}_{\mathbf{III}}(\delta, G) = q\left(\frac{1}{w} + \frac{1}{u_f} - \frac{G}{L}\right) \tag{42}$$

IV. $(L/u_f < \delta < C + L/u_f - G) \cap (\delta > C - L/w + G) = C - L/w + G < \delta < C + L/u_f - G$ The range equation for this region can be found as

$$\mathrm{R}_{\mathbf{IV}}(\delta, G) = q\left(\frac{1}{w} + \frac{1}{u_f} - \frac{2G}{L}\right). \tag{43}$$

These three range equations show that range is independent of δ for given criteria. □

SIMULATION

In the previous section we assumed deterministic values of all parameters (link lengths, green durations, offsets) and no turns. However, real life networks contain some variability in the network parameters and also drivers' decisions contain stochasticity. By introducing a degree of variability, analytical solutions are not anymore obtainable. Thus, we develop a simulation platform to estimate the passing rates and average speeds of forward and backward observers running a series of many intersections with variable characteristics.

While variational theory allows for changes in the network parameters, it does not give the ability to introduce drivers with different characteristics (free flow speed, capacity headway etc) and turning movements. But, we can mimic the effect of driver stochasticity and small amount of incoming turns by adjusting offsets and green durations. For example, consider an arterial's signal plan, which has been designed for a prefect progression, a "green wave", with offsets equal to L/u_f. By introducing some randomness in the offset, e.g. $L/u_f \pm 5$ sec we can imitate the variability in the free flow travel time of the first vehicles in the platoon.

The simulation platform includes a time-space diagram with many links (~1000). The network parameters (lengths, offsets and greens) are specified from the user in the beginning of the simulation in column or matrix forms. (next paragraph continues here, not a new one). After creating the simulation environment, we send different types of observers at the start time of a green phase running at the free flow speed from the upstream in the direction of flow and with the backward wave speed from downstream in the direction against flow. Every observer on the same direction has equal (free flow or backward wave) speeds but they have different behavior than the deterministic case at extended red phases, as there is not a repetitive deterministic pattern (e.g. an observer stop every 3 signals).

In simulation, this pattern becomes stochastic by giving probabilities that an observer will stop if she meets an extended red phase. According to (*1*) an extended red phase is used to make observers stop every $1, 2..., g_{max} - 1$ traffic signals. Each observer, which enters the simulation is assigned with a probability of stopping each time she meets a green phase. Faster observers are assigned with smaller probability and slower observers with higher one. For instance, if the probability assigned to this observer is 0, this observer will only stop when it hits red whereas the observer with probability 1 will stop in every signal. If we consider an observer with probability p, it will pass on green phases with probability $(1 - p)$. For each observer we have to estimate two values, the average speed and the average passing rate. Average speed can be found by dividing

the sum of link lengths to the total travel time. Similarly, we track the number of passing/passed vehicles for each observer during the simulation and divide them by the total travel time. An informal pseudocode for a single forward moving observer can be seen above. The one for the backward moving observer is the same. The only difference is the speed, the start and the direction of the movement:

Note that in the pseudocode given above, green phase matrix $\mathbf{G}$ is represented as a set of unions of real number intervals $\mathbf{G}_i$ to be consistent with mathematical notations. They represent the same parameter set. Figure (3b) shows a time space diagram with the forward and backward observers with different values of stopping probabilities.

Incoming Turns

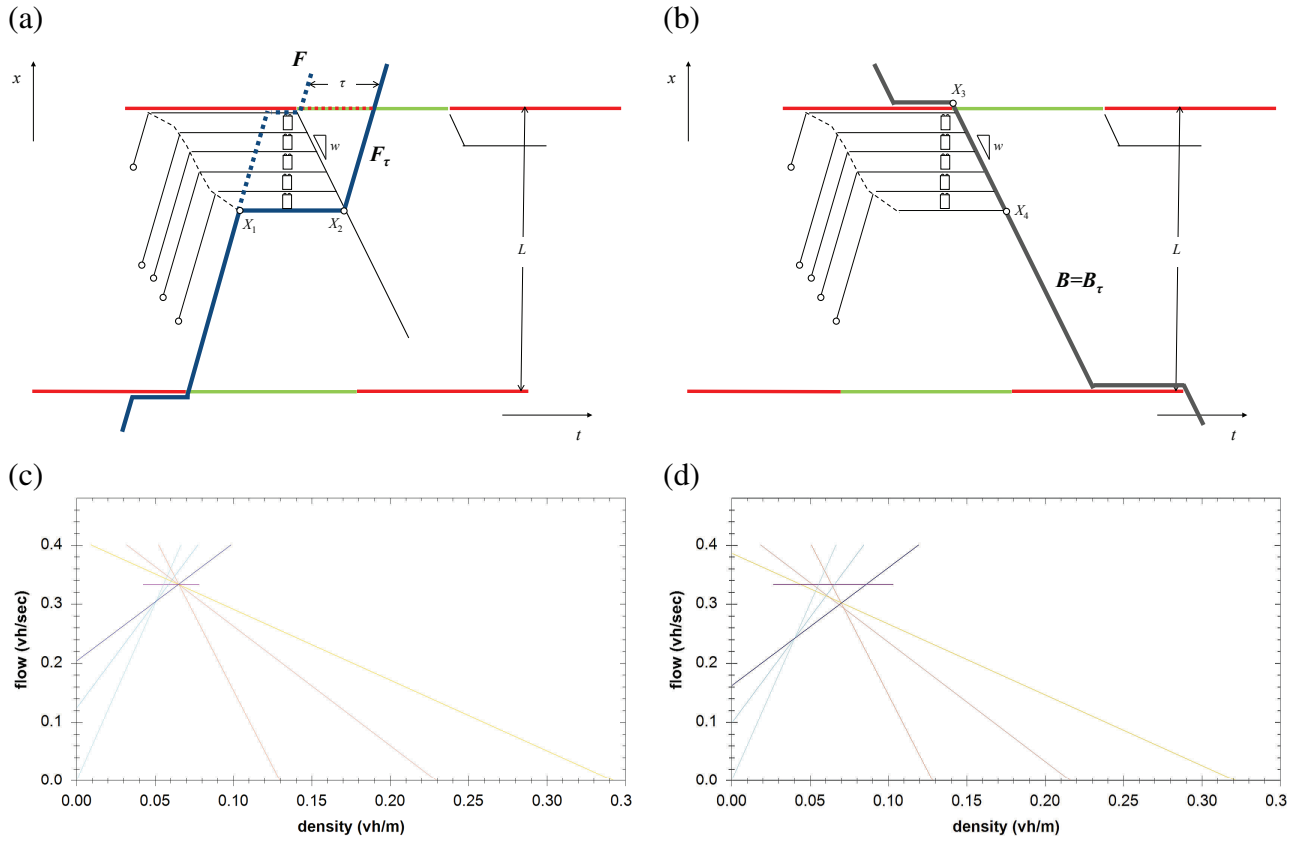

Figure 4: Integrating the effect of incoming turns within VT: Time-space Diagrams for forward and backward moving observers with ($\boldsymbol{F}$ and $\boldsymbol{B}$) and without turns ($\boldsymbol{F}_\tau$ and $\boldsymbol{B}_\tau$).

Reference (*1*) showed that an MFD must arise for single-route networks with a fixed number of vehicles in circulation (i.e., periodic boundary conditions and no turns). The authors also conjecture that the MFD formulae should apply to a network of intersecting routes if the the numbers of vehicles in these routes are similar and roughly constant over time. We now address the effect of incoming turns in a single-route network by introducing bottlenecks of variable capacity in the proximity of the traffic signals.

Incoming turns from cross streets can significantly decrease the performance of a signalized

input: n (number of traffic signals), $\mathbf{l}$ (link length vector), $\mathbf{G}_i$ (green set for signal i), p (extended red phase probability) and u_f (free flow speed)
output: v (average speed) and PR (average passing rate)

1. Set time t to first green signals start time t_0 and total passing rate TPR to 0.
2. Repeat if current traffic signal counter $i < n$
   (a) Advance the time by travel time on that link: $t \leftarrow t + \frac{L[i]}{u_f}$
   (b) Update the current traffic signal counter $i \leftarrow i + 1$.
   (c) If it hits a green ($t \in \mathbf{G}_i$)
      i. If it is an extended red phase ($p >$ RAND $(0, 1)$)
         A. Find extended red phase duration k.
         B. Update total passing rate: $TPR \leftarrow TPR + kq$
         C. Advance time t to next green.
      ii. If it is not an extended red phase ($p \leq$ RAND $(0, 1)$)
         A. Do nothing.
   (d) else if hits a red ($t \notin \mathbf{G}_i$)
      i. Advance time t to next green.
3. Calculate the average speed $v \leftarrow \frac{\sum_{i=1}^{n} L_i}{t - t_0}$ and the average passing rate $PR = \frac{TPR}{t - t_0}$

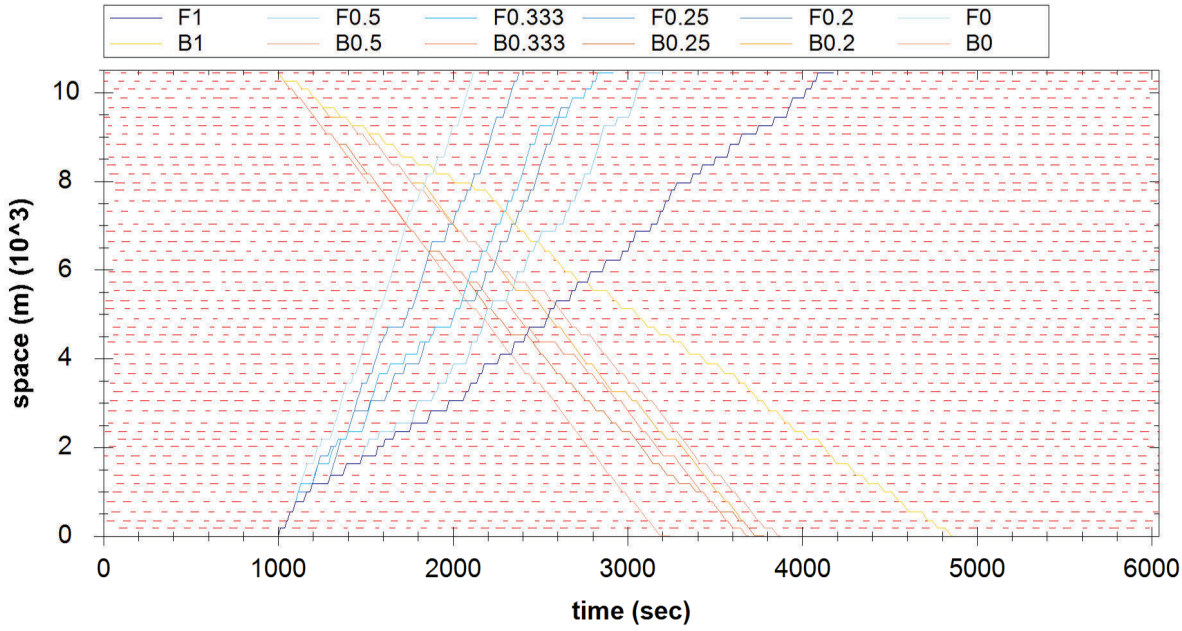

Figure 3: Simulation platform: (a) pseudocode (b) time-space diagram

intersection as they (i) interrupt the progression of green waves for properly timed signals and (ii) decrease the available storage capacity of the link and can cause the occurrence of spillbacks. We address the above phenomena by changing the signal and cost function characteristics for forward and backward moving observers. To be consistent with variational theory, these turns should not significantly change the link density from one link to another, i.e. the incoming turns are considered as local link phenomena and these vehicles do not advance in the downstream links.

Consider now a queue of incoming vehicles from cross streets, Q, which entered when the signal was red for the through movement (Figure (4a)). If these vehicles did not exist a forward moving vehicle would follow trajectory $\boldsymbol{F}$ (Figure (4a)) and would stop for some time at the traffic signal stopline. Because of the queue of incoming turns, the upstream vehicle needs to stop between points X_1 and X_2, follow trajectory $\boldsymbol{F}_\tau$ and cross the intersection τ seconds later, where $\tau = sQ$. According to variational theory the cost (passing rate) of a forward moving observer who stops in the middle of a link between X_1 and X_2 is $s*$(*duration of stop*). But, in reality no vehicles can overpass this observer while stopping, because in front of him there is a queue of vehicles entered from a cross street. Thus, we imitate this effect by increasing the red phase of the signal by τ. Thus, a forward moving observer in the simulation will follow trajectory $\boldsymbol{F}_\tau$ instead of $\boldsymbol{F}$. But, this extended red in the beginning of the green has passing rate 0 and not s. Nevertheless, the stationary observer in front of the traffic signal continues to count vehicles for the whole duration of the real green phase as the incoming turns are served in the first τ seconds of green.

For the backward moving observer, $\boldsymbol{B}_\tau$ (Figure (4b)) our approach is slightly different. This observer does not need to stop in the extended red phase of τ seconds. But when traveling backwards between points X_3 and X_4, its passing rate is not r, but 0. Thus, the queued vehicles from cross street, give her the ability to travel in this queue with zero cost.

Based on the above, for forward moving observers both the speed and passing rate decreases, for backward moving observers only the passing rate decreases, while for stationary observers there is no change. Thus, tighter cuts are created which can decrease both the range and the capacity of the MFD. An example is shown in Figure (4c and d) with and without turning effects. Analysis of the results is provided in the next section.

RESULTS

In this part, we firstly investigate the deterministic cases which is solved by the analytical formulae given in "Deterministic" section and then continue with the simulation results. As it is defined in Figure (1a), capacity is the ratio of the maximum flow q_{max} to the flow observed by the stationary observer which equals to sG/C (dimensionless). Range is the the difference between maximum and minimum density which yields the maximum flow q_{max}. Since the value of the negative range does not mean anything and capacity equals to 1 if the range is nonnegative, it is possible to merge contour lines for both range and capacity at the same graph. These merged graphs can be seen in Figure (5)-(6). Note that, blue stands for the range whereas red stands for the capacity.

Deterministic Network Parameters

Figures (5a-d) show how range and capacity change with δ and G/C for three different cases (i) $C = 60sec$, $L = 110m$, (ii) $C = 120sec$, $L = 180m$ and (iii) $C = 90sec$, $L = 225m$. The white area between the blue and red isoquants represents scenario with capacity 1 and range 0, i.e. tightest forward and backward observers intersect with the stationary one at the same point. Note for a range of δ (e.g. $8 - 38sec$ in figure (5a)), density range is invariant with offset. Note also that

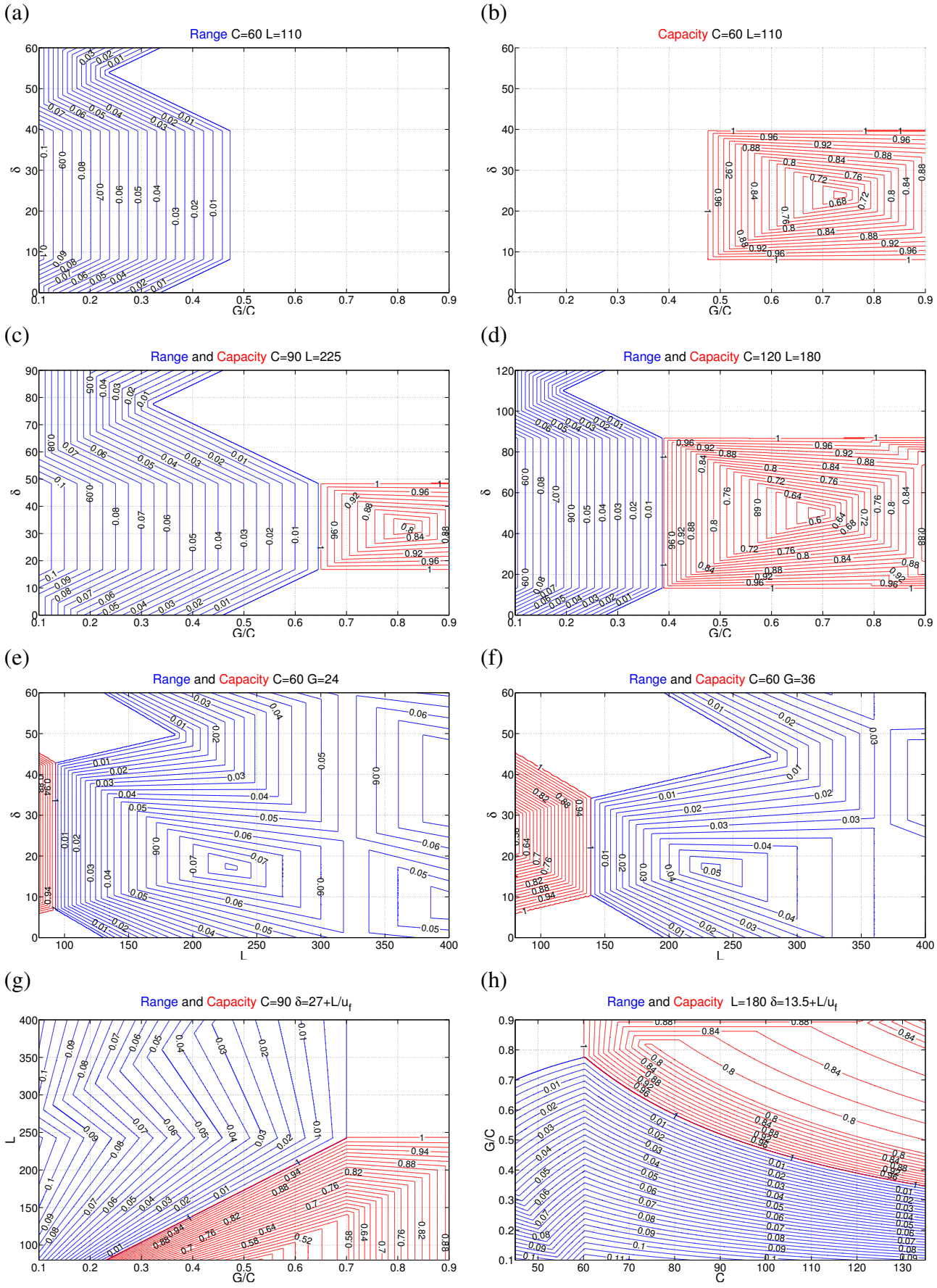

Figure 5: Deterministic

by increasing G/C after some value, it does not increase the number of vehicles that can be served per cycle (remember that the graphs show dimensionless capacity). Note also that the effect of bad coordination in the capacity of a short link is much more significant in case of short links and when the cycle is longer (compare figures (5c) with (5d)). Notice that not only perfect coordination in offset (L/u_f) but also the values between L/u_f and $C - L/w$ gives the maximum range for any given G/C ratio. Furthermore, in this region, range is independent of the offset which was also proved in Section 4. Certainly, the positive range region is larger either when L is larger or C is smaller. This fact can be expected from the Equations (41-43).

Figure (5e-f) show the effect of the length on range and capacity. Range is increasing as the length increases in both graphs. Note that for the same value of offset, as G increases range decreases, as the stationary observer has a higher passing rate value. When L is large, capacity is always 1 for any value of offset. In this case, we can choose offset in a way to maximize the range, as this means that the signal can operate at capacity for a wide range of densities. Also, values in the white regions might not be stable as small changes in demand can create spillbacks or capacity decrease.

In figures (5g-h), we investigate the effect of length, green phase and cycle duration in case of bad offsets (vehicles have to stop in every signal). Note that the boundary line for capacity less than 1, is a piecewise linear function of L and G/C (5g). For example for $L = 150m$, G/C ratio greater than 0.43, will cause not full utilization of signal capacity. Figure (5h) shows the boundary line as a function of cycle and green duration for a given link length. For example for $C = 90sec$, by increasing G/C from 0.5 to 0.7 (40% increase) the improvement in the maximum number of vehicles that can be served is too small (10% increase), $0.25vh/sec$ vs. $0.28vh/sec$ (the values have been obtained by multiplying the numbers of the graph with sG/C). This possibly means that the additional G/C can be utilized to serve cross streets with less delays.

Stochastic Network Parameters

We now utilize the simulation platform to identify the effect of variability when compared with the deterministic cases described before. The results presented assume a uniform distribution for offsets, $U(min, max)$ and a triangular distribution for link length $TR(min, max, mode)$. One can apply different distributions if needed. We analyze two sets of variations: (i) the mean value is constant and range of the variable changes and (ii) the range is constant and the mean of the variable changes. The next three subsections present results for variations in the effect of incoming turns link lengths and offsets.

The Effect of Incoming Turns

We now show that incoming turns from cross streets can significantly decrease the performance of a signalized intersection in some cases as they interrupt the progression of properly timed signals and decrease the available storage capacity of the link.

In all graphs of Figure (6) the vertical axes is the amount of incoming turns (expressed as the extended red phase $\tau = sQ$, which is assumed uniform between 0 and an increasing value). The first two graphs on the top show the effect of turns as the variability of offsets increases for good (left graph) and bad (right graph) offsets. In case of almost perfect offsets the effect of turns is very significant because the value of range for zero turns is very small. On the other hand, the bad offsets can absorb a high number of turns without capacity decrease. Notice that the values of the two graphs coincide for $\delta = 90sec$ as this represents the case of random offsets. A signal timing

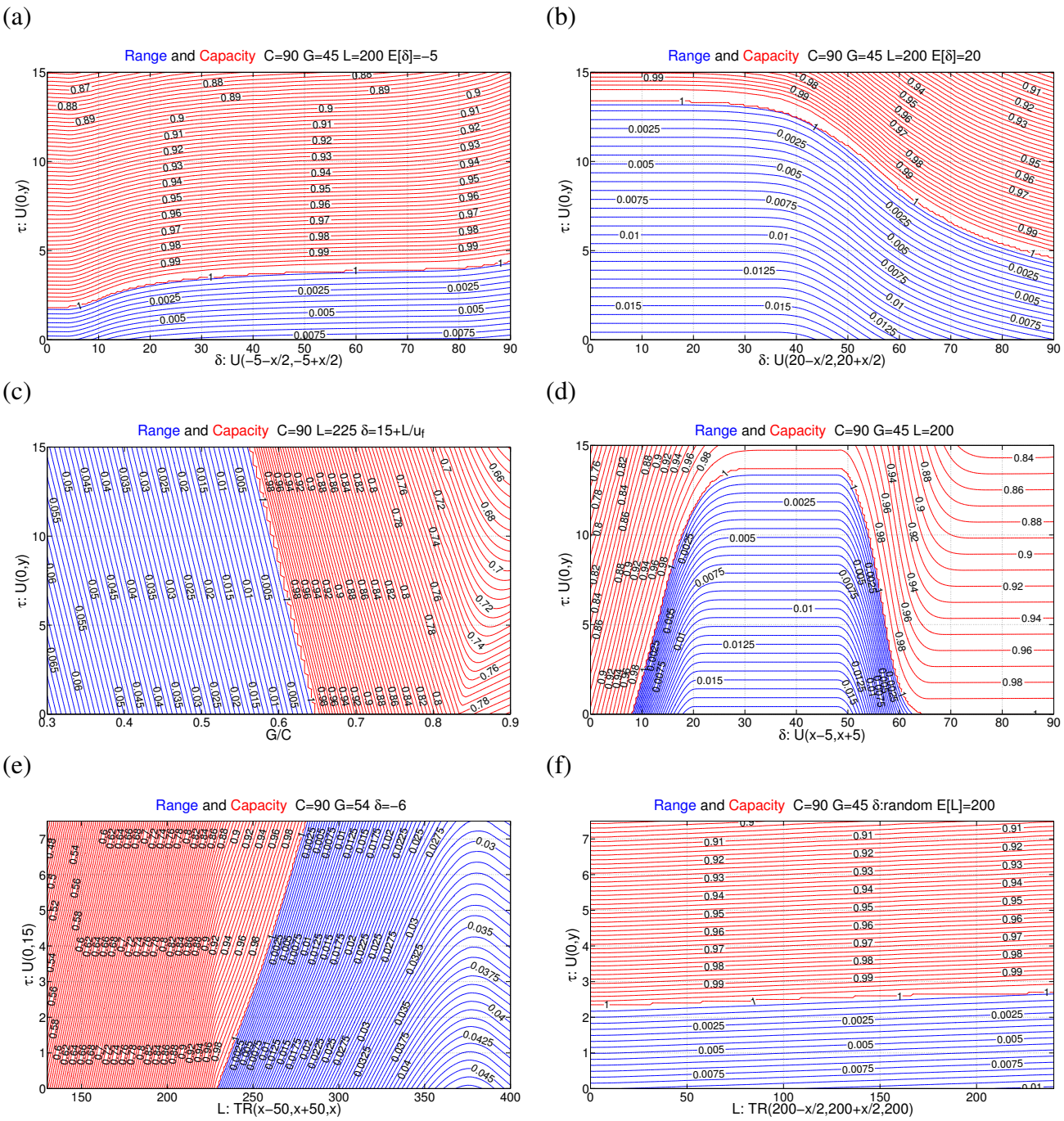

Figure 6: The effect of incoming turns in capacity and range.

with bad offsets can absorb up to 13 seconds of turning (6.5 vehicles), while even one incoming vehicle can create problems for good coordination. But even in case of bad offsets, large G/C is problematic as range is smaller even for 0 turns. Thus, in case of incoming turns, the signal plans should be chosen in a way that maximizes the range as capacity can be significantly decrease. For example in Figure (6d) one can see that a bad offset with higher range is much more robust than a good offset with small range. Of course if signals are undersaturated, they will operate in values much less than capacity and the effect of turns will be minimal. But, in this paper we mainly investigate signal performance in high demand conditions. Also, from Figures (6e-f) it is clear that as length increases the effect of incoming turns becomes smaller because it is more difficult to have queue spillbacks.

Variations in Link Length

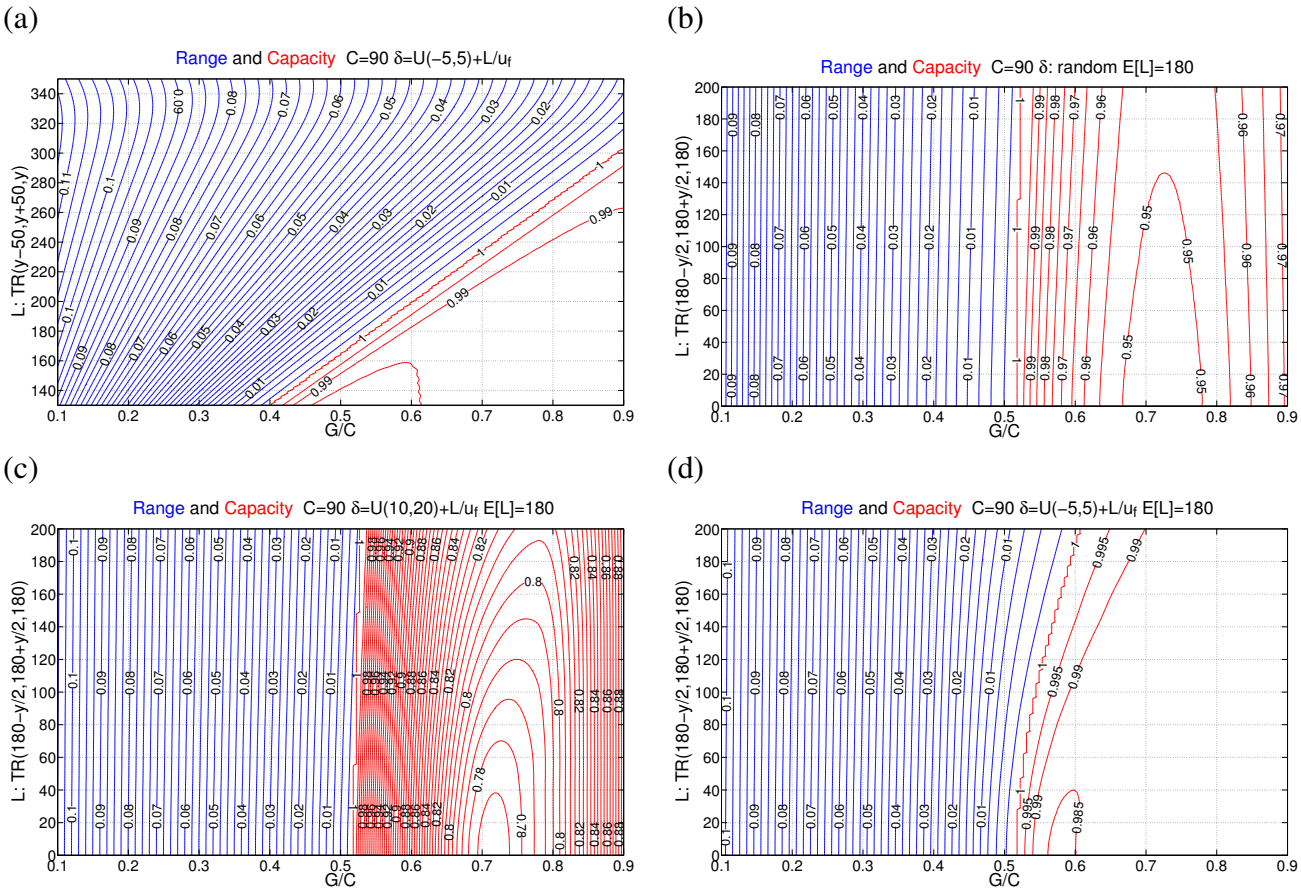

Figure 7: Stochastic L

In the graphs given in Figure (7), both the mean and the variance of the distribution of L is analyzed. In Figure (7a), offset is selected as perfectly coordinated with a small variance and L has a symmetric triangular distribution with constant range of $100m$ and variable mean. It is observed that, the effect of G/C is more if link length is smaller. In other words, shorter link lengths are more sensitive to green ratio. A similar result is obtained if deterministic L is used. Thus, we are interested in identifying the critical length variability which changes the deterministic results.

In the remaining three graphs, the effect of G/C ratio and range of link length is analyzed for links with average length $E[L] = 180$ and three different offsets (perfectly coordinated signals, badly coordinated signals and random offsets). A small variation $\pm 5sec$ has been introduced for good and bad offsets. Figures (7b) to (7d) are intuitive to understand, as vertical isoquants mean that increase in the length variability have no effect in capacity or range. Results show that length variability increase has no effect for values of G/C smaller than 0.45 (capacity is always 1 for these values). But, when capacity is less than 1 there is a range of G/C where significant decrease in capacity is observed for the case of bad offsets. Nevertheless, we observe that when offsets are correlated with the length of the link (this happens in all 3 cases), link length variance has minor effects. For example in case of bad offsets the maximum change is for $G/C = 0.7$, where deterministic $L = 180m$ vs. highly variable L (varying between 80 and $280m$) have a difference in capacity of only 4% (0.78 vs 0.81).

Variations in Offset

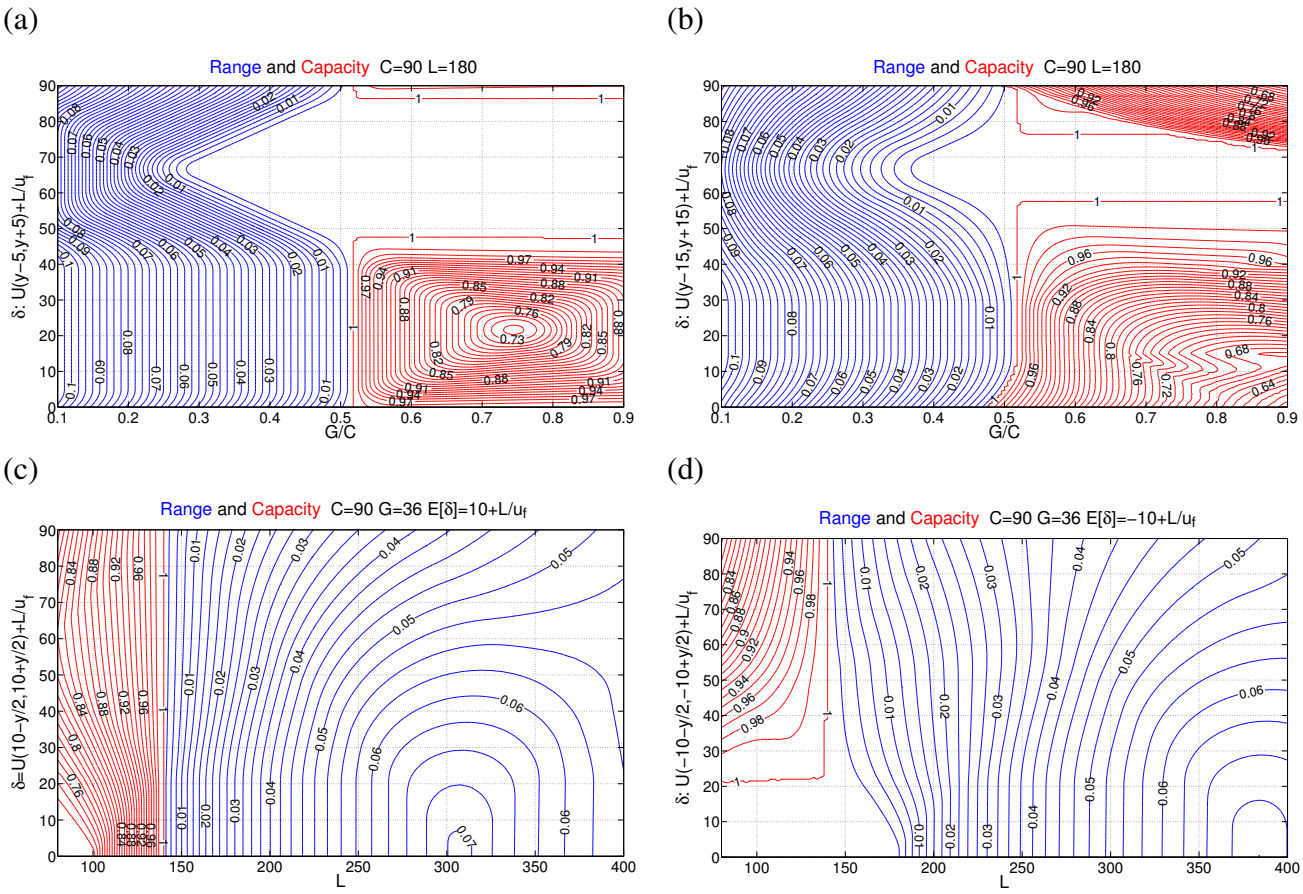

Figure 8: Stochastic δ

We first investigate the effect of small ($\pm 5sec$) and large variation ($\pm 15sec$) in offset by changing mean offset and G/C. The results are summarized in Figures (fig:deltaa and b). If these graphs are compared with the deterministic graphs (Figures (5a-d)), we can say that small offset variations have no significant effect both in capacity and range. This means that small differences in drivers'

characteristics (e.g. free-flow speed, reaction time etc) cannot decrease the performance of traffic signals. However, in case of large offset variations (in case of poorly designed signals) the effect can be significant, especially in regions with capacity less than 1.

In the remaining two graphs, the range of the offset is investigated for good (the first vehicle from upstream arrives $10sec$ after the beginning of green) and bad coordination (the first vehicle arrives $10sec$ before the end of red). All the parameters except the means of the offsets are the same in (c) and (d). When capacity is smaller than 1 (for $L < 140m$), higher offset variability improves the capacity value in case of bad offsets and has a negative effect in case of good offsets. This result is intuitive as more (less) vehicles will hit the green phase during bad (good) coordination. For long links, offset variability decreases the range as for a given L and G/C range is maximized when there are only one forward and one backward observers (Figures (5a-d)).

CONCLUSIONS

In this paper we have provided several extensions and refinements in the Variational Theory of traffic flow, which provides analytical formulae for the Macroscopic Fundamental Diagram of urban networks. In our study we investigated the effect that have in the MFD, different degrees of variability in link lengths and signal characteristics for different city topologies and signal structures. We have integrated the effect of incoming turns in the estimation of the MFD and we showed that in many cases network capacity can significantly decrease. These results can be of great importance to practitioners and city managers to unveil simple and robust signal timing planning in such a way that maximizes the network capacity and/or the density range of the capacity. Ongoing work is utilizing the above findings to develop perimeter control strategies for heterogeneously congested cities. We are also developing analytical formulae for the MFD of cities with multimodal traffic and investigate how redistribution of urban space between cars and more efficient modes can improve passenger network flows.

REFERENCES

[1] Daganzo, C. F. and N. Geroliminis, An analytical approximation for the macroscopic fundamental diagram of urban traffic. *Transportation Research Part B: Methodological*, Vol. 42, No. 9, 2008, pp. 771 – 781.

[2] Godfrey, J. W., The mechanism of a road network. *Traffic Engineering and Control*, Vol. 11, No. 7, 1969, pp. 323–327.

[3] Ardekani, S. and R. Herman, Urban network-wide traffic variables and their relations. *Transportation Science*, Vol. 21, No. 1, 1987, pp. 1–16.

[4] Olszewski, P., H. S. L. Fan, and Y.-W. Tan, Area-wide traffic speed-flow model for the Singapore CBD. *Transportation Research Part A: Policy and Practice*, Vol. 29, No. 4, 1995, pp. 273 – 281.

[5] Mahmassani, H., J. Williams, and R. Herman, Performance of urban traffic networks. In *Proceedings of the 10th International Symposium on Transportation and Traffic Theory* (N. H. Gartner and N. H. M. Wilson, eds.), Elsevier, Amsterdam, The Netherlands, 1987.

[6] Mahmassani, H. S. and S. Peeta, Network performance under system optimal and user equi-

librium dynamic assignments: implications for advanced traveler information systems. *Transportation Research Record*, Vol. 1408, 1993, pp. 83–93.

[7] Daganzo, C. F., A variational formulation of kinematic waves: basic theory and complex boundary conditions. *Transportation Research Part B: Methodological*, Vol. 39, No. 2, 2005, pp. 187 – 196.

[8] Geroliminis, N. and C. F. Daganzo, Macroscopic modeling of traffic in cities. In *86th Annual Meeting of the Transportation Research Board*, Washington, DC, 2007, Paper No. 07-0413.

[9] Geroliminis, N. and C. F. Daganzo, Existence of urban-scale macroscopic fundamental diagrams: some experimental findings. *Transportation Research Part B: Methodological*, Vol. 42, No. 9, 2008, pp. 759–770.

[10] Helbing, D., Derivation of a fundamental diagram for urban traffic flow. *The European Physical Journal B*, Vol. 70, No. 2, 2009, pp. 229–241.

[11] Laval, J. A. and L. Leclercq, Microscopic modeling of the relaxation phenomenon using a macroscopic lane-changing model. *Transportation Research Part B: Methodological*, Vol. 42, No. 6, 2008, pp. 511 – 522.

[12] Wardrop, J. G., Some theoretical aspects of road traffic research. *Proceedings of the Institution of Civil Engineers, Part II*, Vol. 1, No. 2, 1952, pp. 352–362.